

FLOOD MAPPING AND DAMAGE ASSESSMENT OF KAZIRANGA NATIONAL PARK, ASSAM USING MULTI-TEMPORAL SENTINEL-1 SYNTHETIC APERTURE RADAR IMAGES

S. ANANDA KRISHNAN^{a1}, SURYA GANESH^b, S. SUMITH SATHEENDRAN^c AND ABIN VARGHESE^d

^{abcd}Dr. R. Satheesh Centre for Remote Sensing & GIS, School of Environmental Sciences, Mahatma Gandhi University, Kottayam, Kerala, India

ABSTRACT

Efficient monitoring and prediction of floods and risk management for large reservoir is impossible without the use of Earth Observation data from space. One of the most important problems associated with flood monitoring is the difficulty to determine the extent of the flood area as even a dense network of observations cannot provide such information. The flood extent information is used for damage assessment and risk management. The use of optical imagery for flood monitoring is limited by the presence of clouds. In turn, Synthetic Aperture Radar (SAR) measurements from space are independent of daytime and weather conditions and can provide valuable information to monitor flood events. This is mainly due to the fact that smooth water surface provides no return to antenna in microwave spectrum and appears black in SAR imagery. The present study aims to analyze Sentinel-1A SAR data for its potential to map flood extent over the world's Heritage site Kaziranga National Park, Natural Wonder of the World, Assam during the monsoon period of 2017. Level-1 Ground Range Detected (GRD) Sentinel-1 C-band (5.405 GHz) data collected in the Interferometric Wide Swath-(IW) mode were used to develop a procedure for reliable processing of the Sentinel-1 SAR images. Six SAR images have been collected during the period from 21st March 2017 to 26th July 2017. Those series SAR images were utilized to investigate the multi temporal backscatter properties. Based on the backscatter temporal variability, multi-temporal backscatter observations can be used to classify open water body and land.

KEYWORDS: Microwave, Submergence, Synthetic Aperture Radar, Multi-temporal

Floods are among the most frequent natural disasters caused by meteorological phenomena. They regularly cause large number of casualties with increasing economic losses. The conventional means to record hydrological parameters of a flood often fail to record an extreme event. Space technology has made substantial contribution in all the three phases such as preparedness, prevention and relief phases of flood disaster management (NDMA (National Disaster Management Authority Plan) (NDMA-2016). Remote sensing data has been widely used for flood mapping and monitoring. If optical data's utility in flood detection depends on cloud cover, active remote sensing with all-weather monitoring capability and its large coverage is an important tool in flood monitoring (Trinh Le Hung, 2007). Flood monitoring and mapping using Earth Observation (EO) data can help authorities and non-governmental organizations in disaster management and coordination of humanitarian efforts. Data from both optical and microwave sensors can be used for flood mapping. In the age of modern technology, the integration of information extracted through Geographical Information System (GIS) and Remote Sensing (RS) with other datasets provides tremendous potential for identification, monitoring and assessment of flood disaster (Pradhan and Shafie, 2009). Earth observation techniques can contribute to finding out more accurately what causes

floods. Together with flood hazard mapping, earth observation techniques can be used to assessing damage to property, infrastructure and agricultural crops. One of the main characteristics of remote sensing is its capability to generate a large amount of information frequently and spatially, becoming a powerful tool for monitoring changing aquatic environments.

Synthetic Aperture Radar (SAR) systems offer the possibility to operate day and night and they are able to penetrate clouds and rainfall, a feature which is of special importance considering the weather conditions under which flood events usually occur. In the past, data from Moderate-Resolution Sensors like the Advanced SAR (ASAR) on-board ENVISAT have been extensively used while more recently; high-resolution imagery from platforms such as TerraSAR-X and Cosmo-Sky Med has become available. RADARSAT-1 is an operational radar satellite system developed by Canadian Space Agency (CSA) to monitor environmental change and the planets natural resources. RADARSAT-2 is the follow on RADARSAT-1 system co-funded by CSA, with improvements in comparison with RADARSAT-1 includes the high resolution (up to 3m), routine left looking and right looking mode for frequent revisit, selective polarizations with fully polarimetric imaging modes, on-board GPS receivers to improve the real-time

position knowledge and higher downlink power. ALOS PALSAR is the Phased Array type L-band Synthetic Aperture Radar (PALSAR) on the Advanced Land Observing Satellite (ALOS) launched by Japan Aerospace Exploration Agency (JAXA). It has different polarization selections from single, dual to fully polarimetric observations and improved orbit controlling capability that allows the more frequent repeat-pass interferometer applications. However, for global applications, due to the price of high-resolution imagery, free data continue to be important despite of their potentially lower resolution.

After end-of-mission was declared for ENVISAT in April 2012, continuity is expected to be ensured by the Sentinel-1 constellation. The Sentinel-1 mission is expected to deliver a wealth of data and imagery. As the first member of the constellation of two satellites, the Sentinel-1A with C-band was launched on 3rd April, 2014. It has dual-polarization capability (HH+HV or VV+VH) which can provide more ground surface information (European Space Agency. (2017) SENTINEL-1 SAR mission). The Flood extent maps derived from Synthetic Aperture Radar (SAR) data can be a key information source for an effective disaster management, helping humanitarian relief organizations and decision makers to obtain spatially-explicit information about inundated areas in a time- and cost-efficient manner. In comparison to manual or semi-automatic flood mapping approaches often utilized in the framework of rapid mapping activities, automatic SAR-based processing chains can substantially reduce the critical time delay between the delivery of satellite data after a crisis event and the subsequent provision of satellite derived crisis information (e.g. the extent of a flood situation) to emergency management authorities (Twele et al., 2016).

The present study aims to analyze Sentinel-1 SAR data for its potential to map flood extent over the world's Heritage site Kaziranga National Park, Natural Wonder of the World, Assam during the monsoon period of 2017. Level -1 Ground Range Detected (GRD) Sentinel-1 C-band (5.405 GHz) data collected in the Interferometric Wide Swath-(IW) mode were used to develop a procedure for reliable processing of the Sentinel-1 SAR images. Six SAR images have been collected during the period from 21st March 2017 to 26th July 2017. Those series SAR images were utilized to investigate the multi temporal backscatter properties. Based on the backscatter temporal variability, multi-temporal backscatter observations can be used to classify open water body and land.

Floods in Kaziranga & Brahmaputra

During the monsoon season every year the river system originating in the Karbi Anglong & Nagaland Hills and flowing through the Park inundate Kaziranga by overflowing the banks and fill up low lying areas. Brahmaputra River bed have been raised by the 1950 earthquake and the gradual silt deposition in such a way that the runoff from this catchment areas during the monsoon cannot be contained in the existing channels of this river. As a result flood has become an annual feature for Kaziranga. Depending on the intensity of the rain in the catchment areas of the Brahmaputra River and its tributaries in the upper reaches floods of varying intensity are experienced in Kaziranga. Though the annual average rainfall in the entire upper catchment areas of the Brahmaputra River and its tributaries may not differ much in a year the intensity of floods in its basin varies due to the intensity of rain in concentrated spells. Depending on such spells of intensive rains flood may occur a number of times in the same year. In Kaziranga as long as the Brahmaputra River remains below the flood level, the runoff from the river originating in the Karbi Anglong Hills is quickly drained out into it and the park remaining free from floods. But if the Brahmaputra River raises above the flood level the excess water from this river bank flows into the Park through the rivers passing through it. The water from the Brahmaputra River thus enters from the park from Western side through the Diffaloo River and Mori-Diffaloo River. The Southern Boundary of the Park being a low-lying area is then flooded by the overtopping of the banks of the Moridiffaloo River. Thus the areas of the Park under the Baguri Block are the first to be submerged during the flood. The bank of the Diffaloo River is comparatively higher and over topping of this bank takes place only when the flood level of Brahmaputra River rises further. As such the central portion of the park is the area which is submerged later. The Northern part of the park is submerged by the overflowing of the Brahmaputra River itself. From these discussions it is evident that the river Brahmaputra is the cause of flood in Kaziranga National Park. With the gradual receding of water level in the Brahmaputra River the back flow of water in the rivers passing through the park stops and they start flowing to the Brahmaputra River again carrying the discharge and the excess water from the Park. Thus water from the submerged high lands clears up fast. But the low lying areas inside the Park from basins especially around the beels on the Southern Boundary on the western and central part remain under water for a considerable period even after the receding of the flood water from other

places. There are quite a number of chapories (river islands) of various sizes which have been formed by silt depositions. The main channel of the river goes on changing its course every year and the areas of maximum silt deposition and erosion also change accordingly. Thus the Northern Boundary of the park is very much unstable and is subjected to the ravages of the mighty Brahmaputra River. The aforementioned chapories are at present contiguous with the Northern Boundary of the park which are separated by shallow channels of the mighty river during the monsoon and joined through extensive sandy areas during the winter season. The beds of some of the beels and nallahs situated inside the park also are being silted up by the annual floods (Assam Forest-A Short Note 2017).

Disastrous Stage of Flood

Excess water of the river Brahmaputra drains through Kaziranga National Park and finds its way back to the same river with receding level of water in its channels. This drainage spreading in an area of 430 Sq. Km with various rivers, streams, channels, beels and vast areas covering grasslands and tree cover makes the water level to rise at various locations inside the park very slowly giving sufficient time to the animals finding their way to higher grounds inside the park and along the Karbi Anglong foothills. Once this stage is reached and animals are accumulated in large numbers on high grounds, any further sudden rise of water due to external factors, not relating to the normal drainage of Brahmaputra flood water, may result into a disastrous conditions living large scale mortality of animals by drowning. These conditions were reflected in the high flood years of 1988 and 1998. The reason for this situation was studied and it is found that breach in the embankment constructed on eastern side of the Kaziranga National Park (KNP) along river Dhansiri from Dhansirimukh to Dhanbari results in flash flood in KNP where the water level rises rapidly to a great height all along southern and central portions of the Park. This year also, Kaziranga National Park has undergone severe flood situations during the monsoon. As per the reports from Assam State Disaster Management Authority, approximately 62% of the national park has been submerged. It caused the death of some endangered species of animals (ASDMA, Flood Report 2017).

The Present Study

- To delineate the flood extent of Kaziranga National Park during the monsoon in 2017 using SAR based Remote Sensing images.

- To assess the inundated area and the extent of damage under different land use - land cover.

STUDY AREA

Location of Kaziranga National Park

Kaziranga National Park lies in flood plain mighty Brahmaputra and in Indo-Burma Bio-geographical region. Originally notified Kaziranga National Park lies between Latitudes 26°34' N to 26°46' N and Longitudes 93°08' E to 93° 36' E. It is spread over the civil jurisdictions of Nagaon and Golaghat districts in Assam with mighty Brahmaputra River on the north and verdant Karbi Anglong hills on the south. With six number of additions, having separate national park status, and two reserved forests namely, Panbari and Kukurakata reserve forests coming under the administrative control of the Kaziranga National Park, the geographical area then lies between Latitudes 26°33' N to 26°48' N and Longitudes 92°51' E to 93° 39' E including a part in civil jurisdiction of Sonitpur district (Fig.1).

The entire Kaziranga National Park area was formed by the alluvial deposits of the Brahmaputra River and its smaller tributaries, which carry a great amount of silt during the rainy season every year. The riverine area thus formed is colonized by *Saccharum* and other grass species as soon as the landmasses are stabilized. But sometimes, it is observed that before the succession of other pioneer tree species could start on such landmasses, they get eroded. Probably numerous channels of the Brahmaputra river crisscrossing the entire area were once flowing through Kaziranga in the past and in course of time silt depositions and changing course of the Brahmaputra river formed into the 'Beels' (water bodies/lakes) of various sizes and depth. This process of erosion and formation of landmasses are still going on along the Northern Boundary of Kaziranga National Park (Fig. 3) (Assam Forest-A Short Note 2017).

Kaziranga National Park

- The world's largest population of Indian One Horned Rhinoceros and Wild Buffalo
- High ecological density of Tigers
- Significant population of Asiatic Elephant
- The junction of the East Asia /Australia flyway and Indo-Asian flyway exhibits considerable diversity in avifaunal species.
- Transitional and successional example of grassland to forest and floodplain to hill evergreen forest communities.

Kaziranga contains the most important and significant natural habitat for in-situ conservation of biological

Diversity, including those containing threatened species of outstanding universal value from the point of view of science or conservation. The above mentioned criteria made Kaziranga National Park to get inscribed on the world heritage list of “Convention is concerning the protection of the world cultural and natural heritage” in the year 1985.

Some of the unique and significant conservation values of Kaziranga National Park are enumerated here. The largest undisturbed and representative area of Brahmaputra Valley flood plain grassland and forest with associated large herbivores, avifauna and wetland values (including Turtle, Dolphin etc.).

Floods are always considered to be a dreaded period for Kaziranga National Park and its animal life but since last decade the increasing level of multi wave flood is really threatening the future of the Park and not only the Rhino. Due to various reasons, mainly deforestation in the upper catchments area of the Brahmaputra, the intensity of the flood is continuously on the rise. During flood most of the animals including the Rhinos have to migrate from the Park and take shelter on the adjacent high grounds in Karbi Anglong Hills or wherever they may find shelter. These areas are populated and protection of the animals during the period of migration from and back to the Park becomes an uphill task as enforcement network is almost non-existent in such areas. Many animals, especially the deer and particularly the young, old and infirm lose their lives by drowning, poaching or run over by vehicular traffic on the National Highway. Flood is also necessary and beneficial for maintaining the ecology of the grasslands and forests though it has some adverse effect. The gradual rising of the water level and quick recession is undoubtedly beneficial but floods of severe intensity which submerge the entire Park for a prolonged period deprive the animals from food and shelter (Assam Forest- A Short Note 2017).

Table 1: Extent of the present Land use land cover in Kaziranga National Park

LULC Type	Area (Hectare)
Water body	15189.24
Braid bars	26284.84
Grassland	42227.39
Forest	14232.97
Agricultural field	2773.04
Settlement	757.83

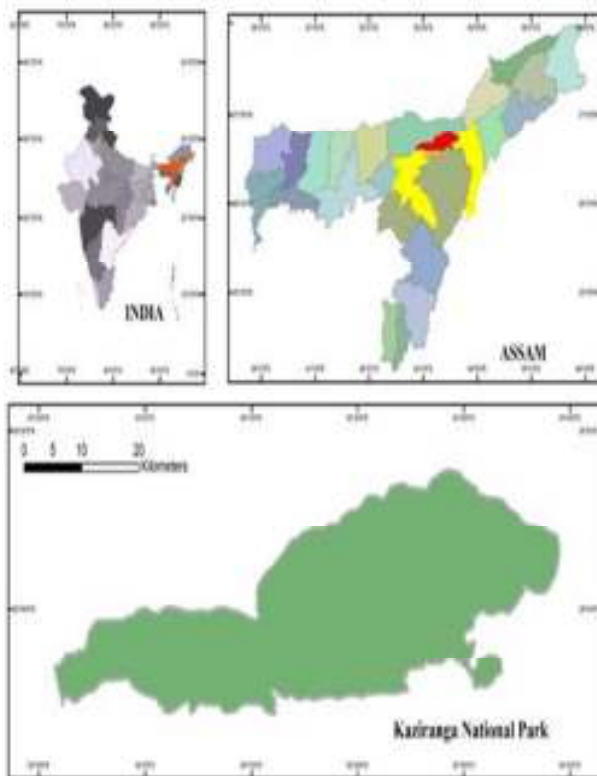


Figure 1: Location Map of Kaziranga National Park

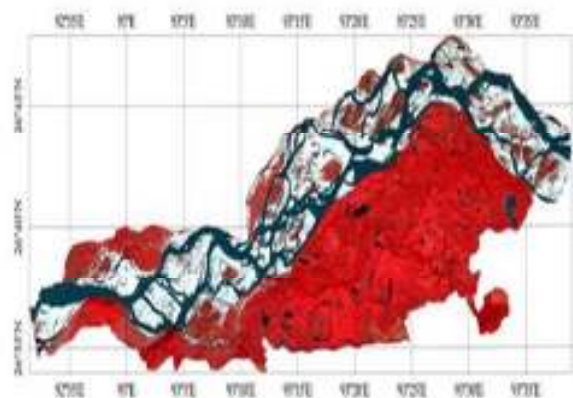


Figure 2: Satellite Image of Kaziranga National Park

(Source: <http://www.assamforest.in/knp-osc/html/images/kaziranga-satellite-view.png>)

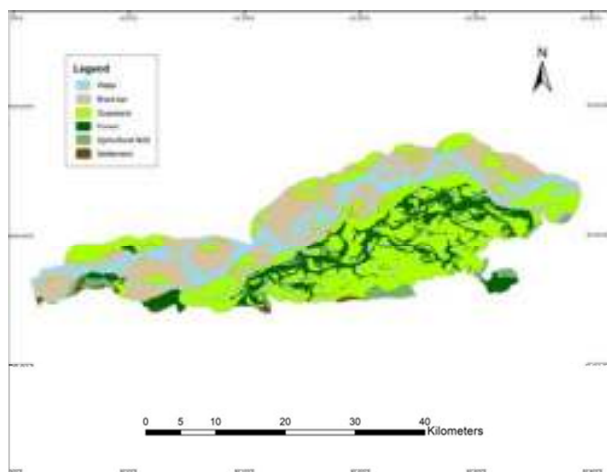


Figure 3: Present Land Use Land Cover of Kaziranga National Park

MATERIALS AND METHODS

Data And Software Used

Sentinel-1 Data

In this study, Level-1 Ground Range Detected (GRD) Sentinel-1 C-band (5.405 GHz) data collected in the Interferometric Wide swath (IW) mode were used. This mode allows the combination of a large swath width (250 km) with a moderate geometric resolution (10m). Images are freely available from the European Space Agency (ESA) through Sentinels Scientific Data Hub (SSDH 2017) (<https://scihub.esa.int/dhus/>). The time interval of the acquired images varies from 5 days up to 11 days. The main characteristics of the collected Sentinel -1 IW data are provided in Table 3. The IW mode is the default acquisition mode over land. The user guide (<https://sentinel.esa.int/web/sentinel/user-guides/sentinel-1-sar>) provides further information on the satellite's acquisition parameters (Table 2).

The polarization of SAR images refers to the geometric plane that the radar wavelength is transmitted and received along. In most systems these are either horizontal (H) or vertical (V) in relation to the satellite antenna, creating four common polarizations: HH, HV, VH, and VV. Although each polarization can be used for flood delineation, the backscatter characteristics of the radar signal varies, impacting the accuracy of the inundation maps produced. Manjusree et al. (2012) compared the four polarizations, concluding that HH has the greatest potential for delineating flooding consistently and accurately, results mirrored in other research (Henry et al., 2006; Brisco et al., 2008). Sentinel-1 collects images in VH and VV polarization when in IW mode, both of which have the potential for classification errors. Cross-polarized data (VH and HV) produces a wider range of backscatter values from vegetated land surfaces compared to co-polarized data (VV and HH), leading to potential overlap with the low backscatter values associated with water, causing misclassification of land as flooded (Manjusree et al., 2012; Twele et al., 2016). VV polarized wavelengths are more susceptible to roughening of the water surface, commonly caused by wind or rain, increasing the backscatter return to the satellite, resulting in inundation not being identified (Manjusree et al., 2012). The limitations of each polarization as environmental conditions vary requires acknowledgement when using Sentinel-1 for flood mapping. Previous research concluded that under calm wind conditions VV provides a slightly higher thematic accuracy than VH polarized data for identifying flooding when using Sentinel-1 data (Twele et al., 2016).

The polarization of SAR images refers to the geometric plane that the radar wavelength is transmitted and received along. In most systems these are either horizontal (H) or vertical (V) in relation to the satellite antenna, creating four common polarizations: HH, HV, VH, and VV. Although each polarization can be used for flood delineation, the backscatter characteristics of the radar signal varies, impacting the accuracy of the inundation maps produced. Manjusree et al. (2012) compared the four polarizations, concluding that HH has the greatest potential for delineating flooding consistently and accurately, results mirrored in other research (Henry et al., 2006; Brisco et al., 2008). Sentinel-1 collects images in VH and VV polarization when in IW mode, both of which have the potential for classification errors. Cross-polarized data (VH and HV) produces a wider range of backscatter values from vegetated land surfaces compared to co-polarized data (VV and HH), leading to potential overlap with the low backscatter values associated with water, causing misclassification of land as flooded (Manjusree et al., 2012; Twele et al., 2016). VV polarized wavelengths are more susceptible to roughening of the water surface, commonly caused by wind or rain, increasing the backscatter return to the satellite, resulting in inundation not being identified (Manjusree et al., 2012). The limitations of each polarization as environmental conditions vary requires acknowledgement when using Sentinel-1 for flood mapping. Previous research concluded that under calm wind conditions VV provides a slightly higher thematic accuracy than VH polarized data for identifying flooding when using Sentinel-1 data (Twele et al., 2016).

Table 2: Sentinel-1 data acquisition modes and resolution

Mode	Access Angle	Single Look Resolution	Swath Width	Polarization
Interferometric Wide Swath	>25 deg.	Range 5m Azimuth 20 m	>250 km >20x20 km	HH+HV or VV+VH
Wave mode	23 deg. and 36.5 deg.	Range 5m Azimuth 5 m	Vignettes at 100 km Intervals	HH or VV
Strip Map	20-45 deg.	Range 5m Azimuth 5 m	>80 km	HH+HV or VV+VH
Extra Wide Swath	>20 deg.	Range 20 m Azimuth 40 m	>250 km	HH+HV or VV+VH

Table 3: Characteristics of the Sentinel-1 Interferometric Wide swath mode nominal measurement modes.

Parameter	Interferometric Wide-swath mode (IW)
Swath width	250 km
Incidence angle range	29.1° - 46.0°
Sub-swaths	3
Azimuth steering angle	± 0.6°
Azimuth and range looks	Single
Polarization options	Dual VV+VH
Maximum Noise Equivalent Sigma Zero (NESZ)	-22 dB
Radiometric stability	0.5 dB (3 σ)
Pixel size (meter)	10

Software Used

- Sentinel Application Platform (SNAP 5.0)
- Quantum-GIS (QGIS 2.18)

METHODS

Sentinel-1 Data Pre-Processing

SNAP software (Sentinels Application Platform) particularly the S-1 Tool box of the SNAP was utilized to pre-process the SAR imagery. SAR data can be accessed by targeting the entire Sentinel ZIP file in SNAP. The original SAR image is inverted in the SNAP. It is displayed according to the order of data acquisition, which is not according- to a cartographic representation. Furthermore, the synthetic method used for creating the SAR imagery also has some disadvantages. Inherent to the measurement technique is random constructive and destructive interference of waves which cause the SAR images to be noisy. This noise within the SAR images is called speckle and decreases the quality of the image and making interpretation of features more difficult. A number of speckle filters types are provided in SNAP. Speckle noise reduction was applied by using single product speckle filter. Speckle filtering is needed to suppress the noise in order to allow better interpretation and backscatter analysis. However, speckle filters not only suppress the noise, but also remove observations that are not affected by noise and contain valuable land surface information (e.g. soil moisture, biomass and flood extent). Here, single product speckle filter method in SNAP was used to remove the speckle. The SNAP S-1 Tool box operator supports the following speckle filter types for handling speckle noise of different distributions (Gaussian, multiplicative or Gamma): Mean, Median, Lee, Refined

Lee, and Gamma-MA. Lee Filter is based on multiplicative speckle model and uses local statistics to preserve details. Lee filter works on the variance basis, i.e. If variance of the area is low then it performs smoothing operation but not for high variance. That means it can preserve details in low as well as in high contrast hence it has adaptive nature (Jyoti Jaybhay and Rajveer Shastri, 2015). Hence the present study used Lee sigma filter with 7x7 window size.

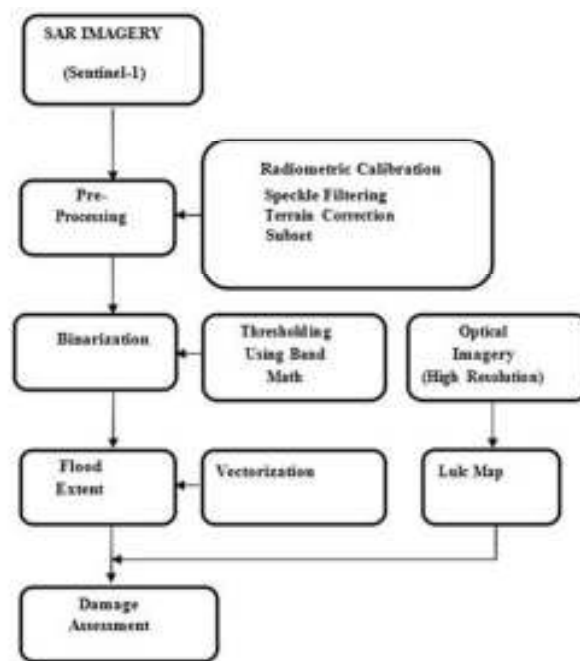


Figure 4: Scheme of Work

To re-project the images from geometry of the sensor to the geographic projection, terrain correction was applied. The Processing Parameters are, Digital Elevation Model (SRTM-1Sec) (Auto Download) DEM over the region that SAR image covers will be automatically downloaded; DEM Resampling Method – Bilinear Interpolation; Image Resampling Method – Nearest Neighbour; Pixel Spacing - 10 m (which is depending on the sensor and its acquisition mode); Map projection - WGS84. Thresholding method is used for delineating water from non-water. For this an average threshold value of 5 SAR images (2.48×10^{-2}) is used to separate water (Fig. 4).

RESULTS AND DISCUSSION

In the analysis dual polarized SAR images from different date were used to detect the flood extent. A one week window between 7th and 14th July was the peak flood period. The rainfall values from nearby stations were also very high.

Table 4: Extent of flooded areas under different land use land cover

Date	FLOODED LULC AREA (HECTARES)					
	Water body	Braid bars	Grassland	Forest	Agricultural field	Settlement
02-07-2017	12917.83	17597.32	8372.59	269.39	240.67	69.67
07-07-2017	14417.27	20410.75	13030.65	511.39	754.61	145.10
14-07-2017	14423.36	19391.49	13775.83	577.80	873.73	193.64
19-07-2017	13853.84	16443.52	8381.06	342.05	457.37	103.83
26-07-2017	13436.58	15844.05	7028.59	263.70	146.43	79.59

Flood adversely affected the different land use and land cover of the National park. It is found that the peak flood event occurred on 14th July. By analyzing the Table 4, it is clear that more area submerged on 7th and 14th July. In the pioneer stage of the flood 20410.75 ha of braid bar submerged out of 26284.84 ha which means 77.65% of braid bars were inundated (Table 4) (Fig. 5 to 10).

As a result of continuous raining of one week, the flood extent drastically increased and the river Brahmaputra started to overflow. The flood water flowed over the lowland of the National park. Which is the favourite grazing land of the animals consists plenty of shorter grasses. On 2nd July, 20% of the total grassland got submerged, whereas after one week it became 33%. As a result, grazing animals may suffered shortage of food. The thick forest areas are comparatively on higher grounds, hence only 4% of forest is flooded. It is also found that 873.73 Hectare of Agricultural field got submerged. During this time flood caused considerable damage to the Roads, Bridges, Guard camps etc. By 19th and 26th July, the total flooded area gradually decreased from 49235.85 ha (which is 48.52 % of the total park area) to 36798.94 ha (36.26% of the total park area).

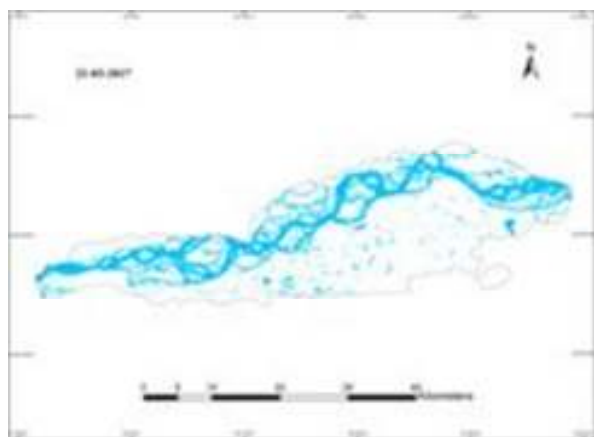


Figure 5: Reference map on 21-March-2017

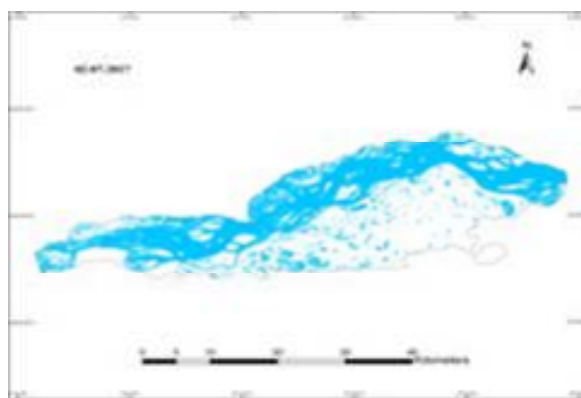


Figure 6: Flood map on 02-July-2017

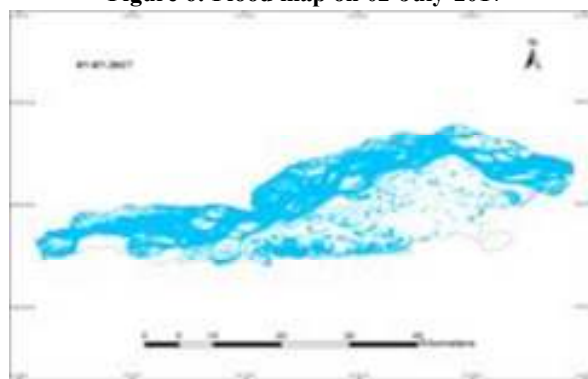


Figure 7: Flood map on 07-July-2017

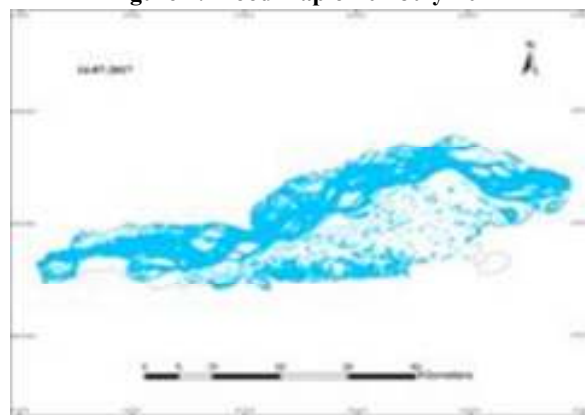


Figure 8: Flood map on 14-July-2017

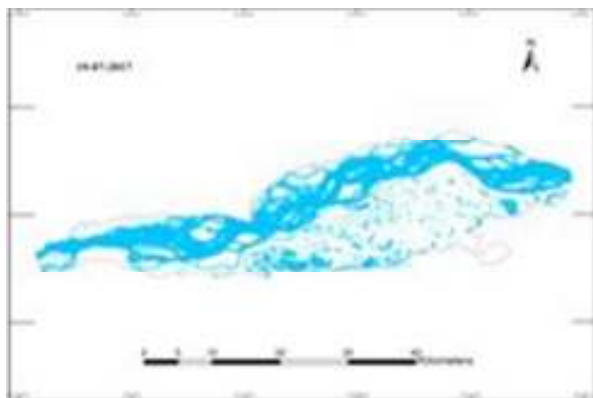


Figure 9: Flood map on 19-07-2017

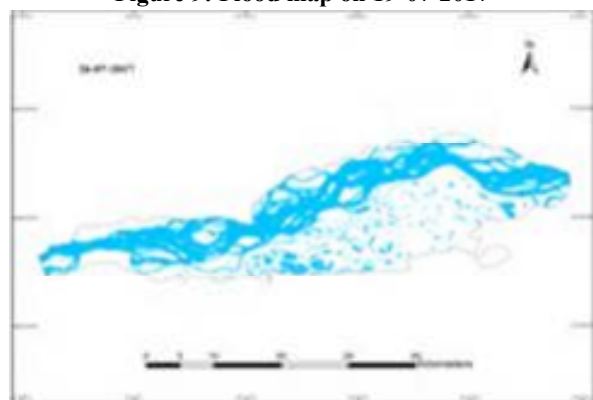


Figure 10: Flood map on 26-07-2017

CONCLUSION

Flood monitoring using SAR data proved to be an effective method to get quick and precise overview of flooded areas. In the study, timely and detailed analysis had been carried out using Remote Sensing & GIS tools for locating & Identifying flooded areas along with land use / land cover features (Mateul Haq et al., 2012). Due to the cloud cover and rain it is very difficult to use optical satellite imagery. It was found that this method requires processed satellite images which were then overlaid with land use land cover map for damage estimation. The methodology used in this study has the capability to carryout rapid damage assessment.

ACKNOWLEDGEMENTS

Many thanks to the authorities of 27th Swadeshi Science Congress held at Amrita University, Kerala.

REFERENCES

ASDMA, Flood Report 2017, Available at www.asdma.gov.in/reports, [Accessed on 12 September 2017].

Assam Forest- A Short Note 2017, Available at <http://www.assamforest.in/knp-osc/pdfreport> [Accessed on 27 July 2017].

Brisco B., Touzi R., van der Sanden J.J., Charbonneau F., Pultz T.J. and D'lorio M., 2008. Water resource applications with RADARSAT-2 – a preview. *International Journal of Digital Earth*, **1**(1):130–147.

Henry J.B., Chastanet P., Fella K. and Desnos Y.L., 2006. Envisat multipolarized ASAR data for flood mapping. *International Journal of Remote Sensing*, **27**:1921–1929.

Jaybhay J. and Shastri R., 2015. “A study of speckle noise reduction Filters”. *Signal & Image Processing: An International Journal (SIPIJ)*, **6**(3).

Manjusree R., Kumar L.P., Bhatt C.M., Rao G.S. and Bhanumurthy V., 2012. Optimization of threshold ranges for rapid flood inundation mapping by evaluating backscatter profiles of high incidence angle SAR images. *International Journal of Disaster Risk Science*, **3**(2):113–122.

Haq M., Akhtar M., Muhammed S., Siddiqui P. and Jillani R., 2012. Techniques of Remote Sensing and GIS for flood monitoring and damage assessment: A case study of Sindh province, Pakistan. *The Egyptian Journal of Remote Sensing and Space Science*, **15**(2):135-141.

NDMA (National Disaster Management Authority Plan)-2016. Available at: <http://ndma.gov.in/images/policyplan/dmplan> [Accessed on 15 September 2017].

Pradhan B., Hagemann U., Tehrany M.S. and Prechtel N., 2014. An easy to use ArcMap based texture analysis program for extraction of flooded areas from Terra SAR-X satellite image. *Computers & Geosciences*, **63**: 34–43.

SSDH. (2017) SENTINEL-1 SAR mission. Available at: <https://sentinel.esa.int/web/sentinel/sentinel-1-sar> [accessed on 4 June 2017].

Hung T.L., 2007. Remote Sensing Techniques for Flood Monitoring Using ENVISAT ASAR Data, pp.47-51.

Twele A., Cao W.X., Plank S. and Martinis S., 2016. Sentinel-1-based flood mapping: a fully automated processing chain. *International Journal of Remote Sensing*, **37**(13):2990–3004.